Performance of lasers containing three, five and seven layers of quantum dots

E.Herrmann, P.M.Smowton, Y.Ning, K.M.Groom, D.J.Mowbray and M.Hopkinson

Abstract: The authors have analysed the performance of quantum dot lasers containing three, five and seven layers of InGaAs quantum dots. At room temperature the threshold current density of devices of length between 320 μm and 2000 μm, with uncoated facets, decreases with device length and is lower for higher layer numbers. They explain this behaviour by analysis of measured modal gain spectra, internal optical mode loss and the temperature dependence of the threshold current density. They find that increasing the number of dot layers can improve device performance because the optical mode loss does not increase while the modal gain at a particular wavelength does increase with more dot layers. However, at low temperatures < 200 K they find that the three-layer structure exhibits the lowest threshold current density for devices of length 550 μm and longer. They conclude that the improved threshold current behaviour of the higher layer number devices at room temperature is not primarily due to intrinsic gain saturation but because the required modal gain can be achieved in high layer number samples with a lower quasi-Fermi level separation and hence a reduced population of higher lying energy states.

It is now well accepted that quantum dot lasers can be made with extremely low threshold current density compared to quantum well devices, e.g. [1]. However, the reduced density of states that facilitate the low transparency current and consequent low threshold current is accompanied by a smaller modal gain than is usual in a quantum well device. It has also been suggested that quantum dot active regions may offer other advantages in particular applications such as for high power output [2] and for widely tunable wavelength sources [3]. In applications demanding laser structures with larger losses—for short cavity lengths and where high reflection coating for the facets is not an option—the modal gain that can be obtained from a single layer of dots is insufficient. In fact we have previously shown that the gain obtained from the quantum dot ground state of a single layer of dots can be insufficient even to overcome the internal optical mode loss [4]. We describe the characterisation of devices incorporating multiple layers of dots designed to operate in the 1 μm wavelength band with uncoated facets and lengths between 320 μm and 3000 μm.

IEE Proceedings online no. 20010745

DOI: 10.1049/ip-opt:20010745

Paper first received 12th June and in revised form 21st September 2001

E. Herrmann and P.M. Smowton are with the Department of Physics and Astronomy, Cardiff University, PO Box 913, Cardiff CF24 3YB, UK

Y. Ning is with the Laboratory of Excited State Processes, Institute of Optics, Fine Mechanics and Physics, Chinese Academy of Sciences, Changchun 130021, China

K.M. Groom and D.J. Mowbray are with the Department of Physics and Astronomy, University of Sheffield, Sheffield S3 7RH, UK

M. Hopkinson is with the EPSRC Central Facility for III-V Semiconductors, Department of Electronic and Electrical Engineering, University of Sheffield, Sheffield S1 3JD, UK

The quantum dot laser structures consist of layers of $In_{0.5}Ga_{0.5}As$ deposited within 10 nm of GaAs at a growth temperature of 500°C. The $In_{0.5}Ga_{0.5}As$ material was deposited at a rate of 0.524 monolayers per second and the transition to three-dimensional growth was observed by reflection high energy electron diffraction (RHEED) after 12 s of deposition, for the initial layers, and up to 1 s earlier for subsequent layers. The GaAs layers are separated by 7 nm of $Al_{0.15}Ga_{0.85}As$. The rest of the waveguide core of the device is made up of $Al_{0.15}Ga_{0.85}As$, which was grown at 600°C, and the total waveguide core width was adjusted to maintain a constant optical confinement factor per layer. This was calculated for two-dimensional layers containing the same volume of material as the quantum dots. The structures were clad with doped $Al_{0.60}Ga_{0.40}As$ layers grown at 640°C. The choice of growth temperature of these layers is a compromise between good quality AlGaAs, which requires high temperatures, and keeping the temperature low enough to avoid significantly affecting the properties of the dots. A schematic diagram of the conduction band profile for the three-layer sample is shown in Fig. 1. The quantum dot size and density were estimated from plan-view transmission electron microscopy measurements on an uncapped structure grown using similar conditions. A dot density of $(5 \pm 1) \times 10^{10}\,cm^{-2}$ and a base dimension of $\sim$20–25 nm were deduced. The samples were also characterised by low temperature ($\sim$10 K) photoluminescence (PL). The spectra for the three samples are shown in Fig. 2. Previous work has shown a narrowing of the linewidth of the PL spectrum and a movement of the peak of the PL spectrum to longer wavelengths as the number of layers is increased. This has been attributed either to surface strain from the initial layer

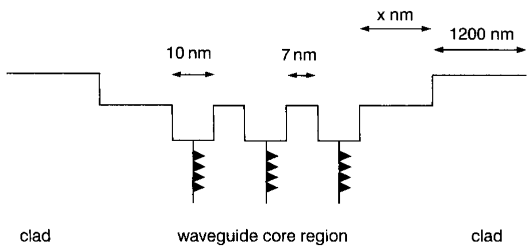

Fig. 1 *Schematic diagram of conduction band profile of 3-layer structure*

▲ position of quantum dots within GaAs quantum wells
Value of x is adjusted from 80 nm to 60 nm to 50 nm when number of layers is increased from three to five to seven to maintain a constant average optical confinement factor per layer

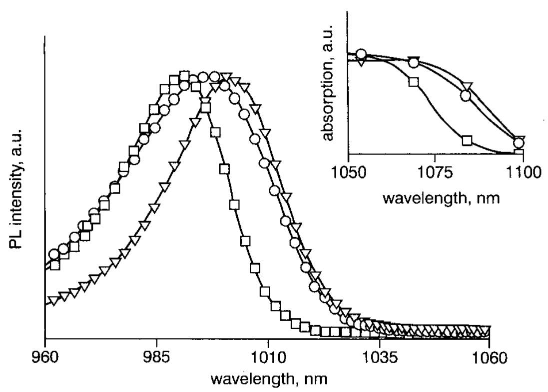

Fig. 2 *Low temperature (≈10 K) photoluminescence (PL) spectra for the three- (○), five- (□) and seven-layer (▽) samples*

Inset shows room temperature photovoltage absorption spectra (PVS)

of dots altering the dot formation kinetics [5] or to electronic coupling between dots in different layers [6]. The full width half maximum (FWHM) of the PL spectra in Fig. 2 do narrow as the number of layers is increased. The width decreases from 49 ± 1 meV for the three-layer sample to 38 ± 1 meV for the five-layer sample to 32 ± 1 meV for the seven-layer sample. The peak of the spectra for the three- and seven-layer samples also follow the expected trend but the peak of the five-layer sample is at shorter wavelengths than the three-layer sample. The reduction in the time for the onset of three-dimensional growth in the latter layers of the high layer number samples is consistent with the initial layers altering the dot formation kinetics, while the effects due to interlayer electronic coupling of the dots themselves are expected to be small because of the large separation between dots in different layers. Clearly a change in the dot formation kinetics after the growth of the first layer is likely to change the emission wavelength of subsequent layers and may affect the gain and other device characteristics. Previous results indicate that such effects can be negligible, with multilayer samples exhibiting the same gain per layer against the current per layer characteristic within experimental uncertainty [7]. To confirm the observed PL results we performed room temperature photovoltage absorption spectroscopy (PVS) [8]. These results are shown in the inset of Fig. 2. The five-layer sample exhibits an absorption 'edge' at a shorter wavelength than the other two samples by ~10 nm, consistent with the PL results. We presume this difference is due to some small variation in the as-grown structures. However, whatever the precise cause, the results presented later in the paper show that the gain spectrum is little changed except for a small wavelength shift.

The structures were fabricated into 50 μm wide oxide isolated stripe lasers with lengths between 320 μm and 2000 μm. Such devices are simple to fabricate and reliable for comparative studies as outlined here. However, it is well known that they tend to produce apparently larger threshold current densities than a ridge waveguide or buried heterostructure lasers, due to effects such as current spreading [9]. Therefore, to allow comparison with the results of other workers we also report threshold current densities for 20 μm wide ridge waveguide devices. The oxide isolated stripe lasers were driven in pulsed mode with a pulse width of 500 ns and a duty cycle of 0.05%. The room temperature threshold current density is plotted against inverse laser length for the three-, five- and seven-layer devices in Fig. 3. The threshold current density varies from ~150 A cm^{-2} for the 2000 μm long devices to ~1000 A cm^{-2} for the 320 μm long three-layer devices. Measurements on the 20 μm wide ridge waveguide devices fabricated from the same wafer resulted in room temperature threshold current densities of ~100 A cm^{-2} for 2000 μm long seven-layer lasers and 60 A cm^{-2} for 3000 μm long devices. The quantity of current spreading implied by the current density results for the ridge waveguide and oxide isolated stripe devices is of the right order according to the Yonezu model [9, 10], where we assume that all the current spreading occurs in the p-GaAs cap layer (with a measured p-doping level of $1 \times 10^{+19}$ cm^{-3}, a literature value of hole mobility of 50 $cm^2 V^{-1} s^{-1}$ [11] and an assumed diode ideality factor of 2). The threshold current densities of the 2000 μm long devices at room temperature, shown in Fig. 3, are similar irrespective of layer number, whereas for shorter devices the three-layer results are significantly poorer than either the five- or seven-layer lasers. To investigate the origin of this behaviour we have measured the internal optical mode loss and the net optical modal gain using a single pass multi-section technique [12]. We have derived values of α_i from measurements of the spectrum of the total modal loss (dot absorption and α_i) for each of the multi-layer samples [7]. The value of α_i measured was 11 ± 2 cm^{-1} for the three- and five-layer samples and 7 ± 2 cm^{-1} for the seven-layer sample. The inclusion of extra layers of dots (and the wells in which they are grown) and the corresponding increase in the number of interfaces does not lead to an increase in the measured optical loss. Having independently measured the values of α_i, we determined the net

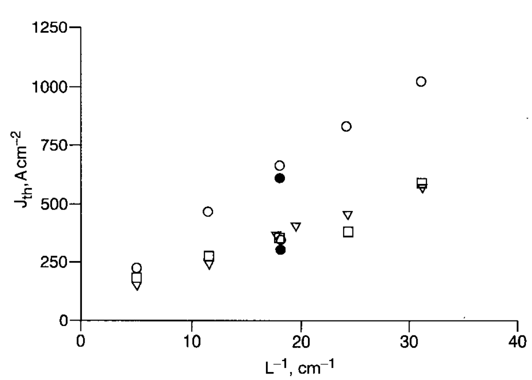

Fig. 3 *Threshold current density against inverse laser length for the three- (○), five- (□) and seven-layer (▽) devices*

Solid symbols are values inferred from gain measurements

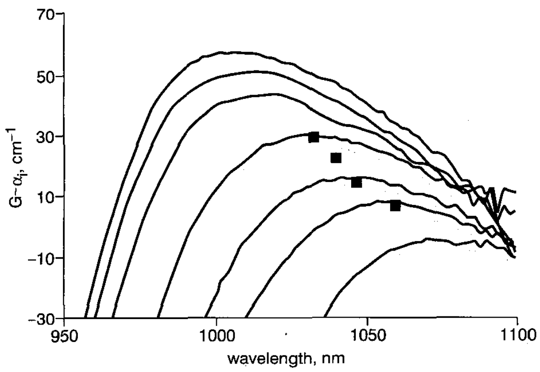

Fig. 4 *Net modal gain spectra for seven-layer sample with applied currents between 139 A cm^{-2} and 1667 A cm^{-2}*

■ calculated mirror loss plotted against lasing wavelength for devices of length 320 μm, 550 μm, 865 μm and 2000 μm

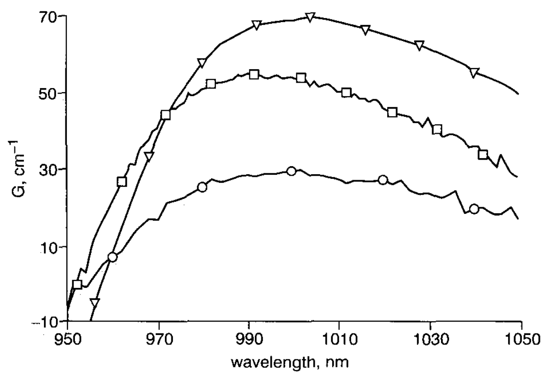

Fig. 5 *Modal gain spectra for the 3- (○), 5- (□) and 7-layer (▽) samples at a constant injection current density per layer of 278 A cm^{-2}*

Horizontal line indicates transparency point. All three characteristics cross this line at the same wavelength (energy) within experimental error

modal gain ($G - \alpha_i$) by using the multi-section device method for the different dot laser structures. The net modal gain spectra for the seven-layer sample with applied currents between 139 A cm^{-2} and 1667 A cm^{-2} are plotted in Fig. 4. As we have previously observed for both a single dot layer sample [4] and multi-layer samples [7], the peak of the net gain spectrum moves to shorter wavelengths with increasing current injection. In addition, each gain spectrum covers a large range of wavelength, as might be expected given the broad low temperature PL spectra of Fig. 2. Both results reflect the inhomogenous broadening of the dot states, which also means that the ground and excited states are not well defined in Fig. 4. The net modal gain is the gain available to overcome the mirror loss and so we have plotted the mirror loss for lasers of length 320 μm, 550 μm, 865 μm and 2000 μm against the measured lasing wavelength in Fig. 4. These plotted laser values coincide with the peak gain and wavelength of the gain spectra and are all at values of loss corresponding to net modal gain produced by the ground state of the quantum dots [7]. The gain spectrum measured as a function of carrier density is central to laser operation and, as such, is the best characteristic to assess the impact that the small variations, observed in the PL and PVS results of Fig. 2, have on device performance. In Fig. 5 we compare the modal gain (G) spectra—having added the measured values of α_i to the net gain spectra of the three-, five- and seven-layer samples at a constant injection current density per layer of 278 A cm^{-2}. Comparing these results (at the same current density per layer) is equivalent to a comparison at the same carrier density per layer only if a number of assumptions are satisfied. First, it is necessary that the proportion of recombination occurring within the dots, the wetting layers or the GaAs quantum wells is the same in each sample. Second, we require that the radiative and nonradiative lifetimes within a layer (dots, wetting layer and quantum well) is the same in all the samples, and finally that all the layers are equally pumped. The spectra of Fig. 5 show that the transition from gain to absorption—the transparency point—occurs at the same wavelength, within the experimental uncertainty, for all three spectra. This shows that any differences between the samples have a negligible effect on the results and provides evidence that the assumptions are being met to this extent. Previous work on a single dot layer sample has indicated that the carriers in different dots are in quasi-equilibrium and can be described by quasi-Fermi levels down to a temperature of 100 K [13]. For this work, carried out at 300 K, it is therefore possible to interpret the transparency point as the quasi-Fermi level separation. Since the quasi-Fermi level separations are approximately the same in Fig. 5 at the same current density per layer, this implies that the structures also have approximately the same carrier population per layer. The gain spectra for all three samples are similar in shape and in gain per layer for the same current density per layer. The peak modal gain increases in the ratio three : five : seven in Fig. 5 within experimental uncertainty. The peak gain wavelength is approximately 10 nm shorter for the five-layer sample, as might be expected given the PL and PVS data of Fig. 2, but the value of gain and the gain spectrum shape do not appear to be significantly different. Neither do the relative amplitudes of the peaks of the gain spectra appear to be significantly affected by the change in dot formation kinetics between the first and subsequent layers. This is presumably because such changes are small compared to the broadening due to dot size fluctuations.

To achieve the same total modal gain in the three-layer as in the seven-layer sample would require a much larger current per layer and results in a blue shift in peak gain wavelength relative to the seven-layer sample. For higher gain values this cannot be achieved without moving the

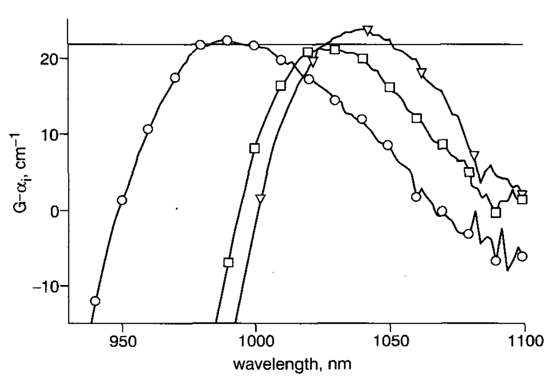

Fig. 6 *Net modal gain spectra where the drive current has been adjusted to provide a maximum gain of ~22 cm^{-1} (solid line), which is sufficient to overcome the mirror losses and produce lasing in a 550 μm long device*

○ three-layer sample
□ five-layer sample
▽ seven-layer sample

peak gain to higher lying states and eventually the wetting layer. In Fig. 6 the net modal gain spectra for the three-, five- and seven-layer samples are plotted where the drive current has been adjusted to provide a maximum gain of $\sim 22\,cm^{-1}$ (solid line). This value of net gain is sufficient to overcome the mirror losses and produce lasing in a 550 μm long device. The values of current density necessary to achieve these gain values are plotted in Fig. 3 and are similar to the threshold current values measured for 550 μm long devices, as would be expected. The quasi-Fermi level separation, as derived from the wavelength at which the net gain $(G - \alpha_i) = -\alpha_i$, occurs at shorter wavelength (has higher energy) for the lower layer number devices, particularly the 3-layer device. This means that higher lying energy states, including the wetting layer states, have a higher probability of being occupied in lower layer number devices.

In Fig. 7 the threshold current density is plotted as a function of heat sink temperature for the three-, five- and seven-layer oxide isolated stripe lasers of lengths 2000 μm and 550 μm. In both cases the threshold current density increases with temperature, exhibiting an exponential type increase at high temperatures, particularly for the low layer number and shorter devices. Such behaviour is typical of a thermally activated loss process which dominates the total recombination current when the quasi-Fermi level separation is large or at high temperatures. This loss process could be due to the population of the wetting layer or the GaAs quantum well and appreciable radiative or nonradiative recombination there. In Fig. 7 at temperatures below ~200 K the three-layer sample has the lowest threshold current density, suggesting that, in the absence of the thermally activated process, the intrinsic gain saturation is not significant (at least for devices of length 550 μm or longer) and the lower transparency current of the three-layer structure can be beneficial.

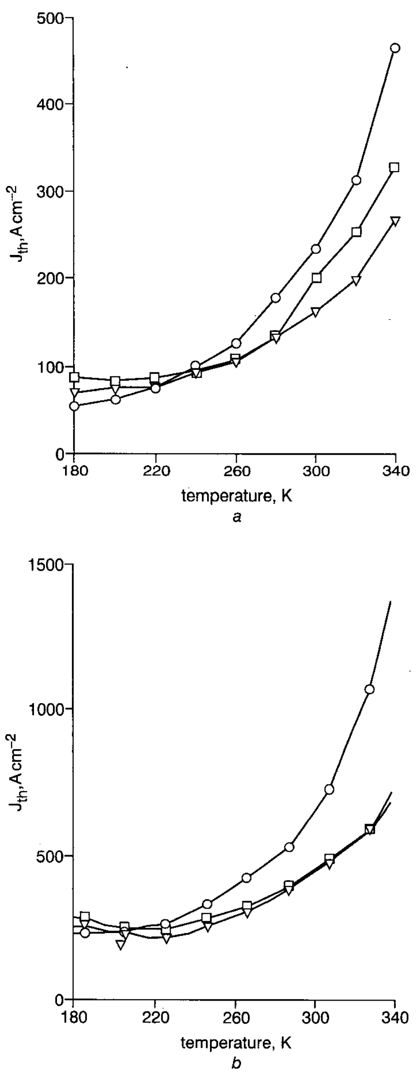

Fig. 7 *Threshold current density against temperature for oxide isolated stripe lasers of lengths 2000 μm and 550 μm*

a 2000 μm
b 550 μm
○ three-layer
□ five-layer
▽ seven-layer

In summary, we have analysed the performance of quantum dot lasers containing three, five and seven layers of InGaAs quantum dots. At room temperature the threshold current density of devices of length between 320 μm and 2000 μm, with uncoated facets, decreased with device length and with increasing layer number. Increasing the number of dot layers can improve device performance because a larger maximum modal gain at a particular wavelength can be obtained without an increase in the optical mode loss. At temperatures below 200 K the three-layer structure exhibited the lowest threshold current density for devices of length 550 μm and longer, suggesting that intrinsic gain saturation is not the primary limitation. The form of the threshold current against temperature characteristic suggested the onset of a thermally activated leakage process at high temperatures.

Acknowledgments

The authors would like to thank Paul Hulyer for fabricating the oxide stripe and Geoff Hill for fabricating the ridge waveguide devices. E.H. and K.M.G. are supported by the UK Engineering and Physical Sciences Research Council.

References

1 LIU, G.T., STINTZ, A., LI, H., MALLOY, K.J., and LESTER, L.F.: 'Extremely low room-temperature threshold current density diode lasers using InAs dots in $In_{0.15}Ga_{0.85}As$ quantum well', *Electron. Lett.*, 1999, **35**, (4), p. 1163

2 GRUNDMANN, M., HEINRICHSDORFF, F., LEDENTSOV, N., RIBBAT, C., BIMBERG, D., ZHUKOV, A.E., KOVSH, A.R., MAXIMOV, M.V., SHERNYAKOV, Y.M., LIFSHITS, D.A., USTINOV, V.M., and ALFEROV, Zh.I.: 'Progress in quantum dot lasers: 1100 nm, 1300 nm, and high power applications', *Jpn. J. Appl. Phys.*, 2000, **39**, pp. 2341–2343

3 VARANGIS, P.M., LI, H., LIU, G.T., NEWELL, T.C., STINTZ, A., FUCHS, B., MALLOY, K.J., and LESTER, L.F.: 'Low-threshold quantum dot lasers with 201 nm tuning range', *Electron. Lett.*, 2000, **36**, (18), pp. 1544–1545

4 HERRMANN, E., SMOWTON, P.M., SUMMERS, H.D., THOMSON, J.D., and HOPKINSON, M.: 'Modal gain and internal optical mode loss of a quantum dot laser', *Appl. Phys. Lett.*, 2000, **77**, pp. 163–165

5 HEITZ, R., KALBURGE, A., XIE, Q., GRUNDMANN, M., CHEN, P., HOFFMANN, A., MADHUKAR, A., and BIMBERG, D.: 'Excited states and energy relaxation in stacked InAs/GaAs quantum dots', *Phys. Rev. B*, 1998, **57**, pp. 9050–9060

6 SOLOMON, G.S., TREZZA, J.A., MARSHALL, A.F., and HARRIS, J.S.: 'Vertically aligned and electronically coupled growth induced InAs islands in GaAs', *Phys. Rev. Lett.*, 1996, **76**, pp. 952–955

7 SMOWTON, P.M., HERRMANN, E., NING, Y., SUMMERS, H.D., BLOOD, P., and HOPKINSON, M.: 'Optical mode loss and gain of multiple layer quantum dot lasers', *Appl. Phys. Lett.*, 2001, **78**, pp. 2629–2631

8 SMOWTON, P.M., BLOOD, P., MOGENSEN, P.C., and BOUR, D.P.: 'Role of sublinear gain-current relationship in compressive and tensile strained 630 nm GaInP lasers', *Int. J. Optoelectron.*, 1995, **10**, pp. 383–391

9 CASEY, H.C., and PANISH, M.B.: 'Heterostructure lasers—Part B: Materials and operating characteristics' (Academic Press, New York, 1978)

10 YONEZU, H., SAKUMA, I., KOBAYASHI, K., KAMEJIMA, T., UENO, M., and NANNICHI, Y.: 'A GaAs-Al_xGa_{1-x}As double heterostructure planar stripe laser', *Jpn. J. Appl. Phys.*, 1973, **12**, pp. 1585–1592

11 BLAKEMORE, J.S.: 'Semiconducting and other major properties of gallium arsenide', *J. Appl. Phys.*, 1982, **53**, (10), pp. R123–R181

12 THOMSON, J.D., SUMMERS, H.D., HULYER, P.J., SMOWTON, P.M., and BLOOD, P.: 'Determination of single pass optical gain and loss using a multisection device', *Appl. Phys. Lett.*, 1999, **75**, pp. 2527–2529

13 SUMMERS, H.D., THOMSON, J.D., SMOWTON, P.M., BLOOD, P., and HOPKINSON, M.: 'Thermodynamic balance in quantum dot lasers', *Semicond. Sci. Technol.*, 2001, **16**, pp. 140–143